

BFA treatment, making them even easier to identify (Fig. 3, asterisks).

The partitioned matrix components were next tested for functionality. NRK cells that had entered metaphase in the presence of BFA were microinjected with a plasmid encoding the plasma membrane marker CD8 (28). After mitosis, BFA was washed out to permit repopulation of the Golgi matrix with enzyme-containing membranes. Two hours later, analysis showed that the re-formed Golgi mediated the transport of CD8 to the cell surface (Fig. 1C). As a control, co-injection of Sar1dn (29) prevented exit from the ER, even though the matrix components re-formed a ribbon-like structure.

As an alternative to BFA, we used Sar1dn to fractionate the Golgi apparatus. Synchronized NRK cells were injected with Sar1dn protein 5 to 6 hours before entry into mitosis, to trap the Golgi enzymes in the ER, leaving the matrix proteins behind. Matrix fragments containing GM130 partitioned at all stages of mitosis in a manner almost indistinguishable from that of untreated cells. Partitioning occurred in the absence of ManII, which was present throughout the ER (Fig. 4).

These two experimental methods for separating Golgi enzymes and Golgi matrix proteins emphasize a partitioning mechanism that is independent of the ER. This mechanism depends on Golgi matrix structures rather than the enzyme-containing membranes that normally populate them, which in turn suggests that these membranes are a less important part of the Golgi partitioning process. They could either travel with the matrix structures to the daughter cells (as we would argue) or get there via the ER (as would be argued by others). Thus, the two models are no longer mutually exclusive, and one could imagine that enzymes could take either or both routes. In this context, recent work on budding yeast suggests that the early Golgi is inherited via the ER, whereas the late Golgi is inherited autonomously (30). In the end, it may not matter how the enzymes are inherited, provided that there is accurate inheritance of the Golgi matrix (31).

- vals of synchronized NRK cells (27). Phase and fluorescence images were acquired with a Zeiss Axiovert 100M microscope equipped with an Orca 100 charge-coupled device camera (Hamamatsu, Hamamatsu City, Japan) and quantified with the program Openlab 3.0 (Improvision, Coventry, UK) (32, 33).
15. Monoclonal antibodies used were as follows: NN2C10 (N. Nakamura) and 4A3 (M. Lowe) against GM130, GTL2 against  $\beta$ -1,4 galactosyltransferase (T. Sukanuma), OKT8 against CD8 (F. Watt), TAT-1 against  $\alpha$ -tubulin (K. Gull), 53FC3 against ManII (B. Burke), and 10C3 against KDEL (Stressgen, Victoria, Canada). Polyclonal antibodies used were as follows: GM130 (M. Lowe), mSec31p (F. Gorelick), GRASP65 (Y. Wang), calnexin (A. Helenius), myc (Santa Cruz, Santa Cruz, CA), and PDI (Stressgen). Alexa Fluor-conjugated secondary antibodies and Topro3 iodine were obtained from Molecular Probes (Eugene, OR). Secondary antibodies conjugated to horseradish peroxidase were purchased from Biosource (Camarillo, CA).
  16. For confocal analysis, unsynchronized NRK cells were treated with BFA (5  $\mu$ g/ml) (Epicentre, Madison, WI) for 90 min, fixed in  $-20^{\circ}\text{C}$  methanol, and processed for immunofluorescence microscopy. Triple-labeled images were acquired on a Zeiss LSM510 microscope with a C-Apochromat 63x/1.2w Korr objective using the sequential (tracking) collection mode, and single sections (0.45  $\mu$ m) in the z axis were collected.
  17. J. Seemann, G. Warren, unpublished results.
  18. R. R. Klevecz, *Methods Cell Biol.* **10**, 157 (1975).
  19. HeLa cells stably expressing NAGTI-myc (34) were synchronized with 1 mM thymidine (Sigma) and treated with BFA, and mitotic cells were collected 90 min later by shake-off (78). After homogenization (35), the PCS was centrifuged on a 5 to 25% glycerol gradient [in 10 mM Hepes/KOH (pH 7.4) and 1 mM EDTA] over an 80% sucrose cushion (3, 6). Fractions were collected and membranes were pelleted and processed for Western blot analysis. Alternatively, the PCS was centrifuged for 30 min at 110,000g to separate the membrane and cytosolic components, which were processed for Western blotting. Magnetic beads [Pan mouse immunoglobulin G (IgG) beads; Dynal, Oslo, Norway] coated (or not) with the monoclonal antibody 4A3 against GM130 were incubated with a PCS from mitotic NRK cells, synchronized using thymidine, and isolated by shake-off. Equal

- fractions (10%) of the supernatant and pellet were processed for Western blotting.
20. F. A. Barr, M. Puype, J. Vandekerckhove, G. Warren, *Cell* **91**, 253 (1997).
  21. N. Nakamura et al., *J. Cell Biol.* **131**, 1715 (1995).
  22. P. Marra et al., *Nature Cell Biol.* **3**, 1101 (2001).
  23. S. Yoshimura et al., *J. Cell Sci.* **114**, 4105 (2001).
  24. A. T. Hammond, B. S. Glick, *Mol. Biol. Cell* **11**, 3013 (2000).
  25. A. R. Prescott et al., *Traffic* **2**, 321 (2001).
  26. NRK cells were processed for Epon epoxy resin sections and immunolabelling as described (33).
  27. M. Lowe, N. K. Gonatas, G. Warren, *J. Cell Biol.* **149**, 341 (2000).
  28. Sar1dn was injected into the cytoplasm at 0.7 to 1 mg of protein per ml, together with sheep IgG (Sigma) to identify injected cells (33). Metaphase cells were injected 90 min after treatment with BFA (5  $\mu$ g/ml). To analyze protein transport, metaphase cells were injected with a plasmid encoding CDB (pCDB) (7) or a mixture of Sar1dn protein and pCDB. BFA was washed out after 1 hour, the cells were incubated for 2 hours at  $37^{\circ}\text{C}$ , and cycloheximide (0.1 mg/ml) (Sigma) was added 45 min before fixation.
  29. Plasmids encoding mammalian Sar1dn mutants were kindly provided by W. E. Balch, and proteins were purified as described (9, 36).
  30. O. W. Rossanese et al., *J. Cell Biol.* **153**, 47 (2001).
  31. L. Pelletier, E. Jokitalo, G. Warren, *Nature Cell Biol.* **2**, 840 (2000).
  32. R. Pepperkok et al., *Cell* **74**, 71 (1993).
  33. J. Seemann, E. Jämsä Jokitalo, G. Warren, *Mol. Biol. Cell* **11**, 635 (2000).
  34. C. Rabouille et al., *J. Cell Sci.* **108**, 1617 (1995).
  35. W. E. Balch, J. E. Rothman, *Arch. Biochem. Biophys.* **240**, 413 (1985).
  36. T. Rowe, W. E. Balch, *Methods Enzymol.* **257**, 49 (1995).
  37. We thank J. Shorter, H. Meyer, L. Pelletier, and the Warren/Mellman lab for helpful discussions and K. Zichichi for technical assistance. Funded by a grant from NIH (to G.W.). T.T. was funded by postdoctoral fellowships from the Uehara Memorial Foundation and the Japan Society for the Promotion of Science (for Research Abroad).

15 November 2001; accepted 19 December 2001

## Role of *Escherichia coli* Curli Operons in Directing Amyloid Fiber Formation

Matthew R. Chapman,<sup>1</sup> Lloyd S. Robinson,<sup>1</sup> Jerome S. Pinkner,<sup>1</sup> Robyn Roth,<sup>2</sup> John Heuser,<sup>2</sup> Mårten Hammar,<sup>3</sup> Staffan Normark,<sup>3</sup> Scott J. Hultgren<sup>1\*</sup>

Amyloid is associated with debilitating human ailments including Alzheimer's and prion diseases. Biochemical, biophysical, and imaging analyses revealed that fibers produced by *Escherichia coli* called curli were amyloid. The CsgA curlin subunit, purified in the absence of the CsgB nucleator, adopted a soluble, unstructured form that upon prolonged incubation assembled into fibers that were indistinguishable from curli. In vivo, curli biogenesis was dependent on the nucleation-precipitation machinery requiring the CsgE and CsgF chaperone-like and nucleator proteins, respectively. Unlike eukaryotic amyloid formation, curli biogenesis is a productive pathway requiring a specific assembly machinery.

Bacteria express a variety of cell-surface proteinaceous filaments that can promote colonization of an epithelial surface, entry into host cells, exchange of DNA between bacteria, and development of bacterial communities orga-

nized as biofilms, colonies, or multicellular fruiting bodies. Curli are a class of highly aggregated, extracellular fibers expressed by *Escherichia* and *Salmonella* spp. that are involved in the colonization of inert surfaces and

### References and Notes

1. D. T. Shima, N. Cabrera-Poch, R. Pepperkok, G. Warren, *J. Cell Biol.* **141**, 955 (1998).
2. E. Jokitalo, N. Cabrera-Poch, G. Warren, D. T. Shima, *J. Cell Biol.* **154**, 317 (2001).
3. S. A. Jesch, A. J. Mehta, M. Velliste, R. F. Murphy, A. D. Linstedt, *Traffic* **2**, 873 (2001).
4. J. M. Lucocq, E. G. Berger, G. Warren, *J. Cell Biol.* **109**, 463 (1989).
5. K. J. Zaal et al., *Cell* **99**, 589 (1999).
6. S. A. Jesch, A. D. Linstedt, *Mol. Biol. Cell* **9**, 623 (1998).
7. M. Terasaki, *Mol. Biol. Cell* **11**, 897 (2000).
8. S. R. Pfeffer, *J. Cell Biol.* **155**, 873 (2001).
9. J. Seemann, E. Jokitalo, M. Pypaert, G. Warren, *Nature* **407**, 1022 (2000).
10. T. H. Ward, R. S. Polishchuk, S. Caplan, K. Hirschberg, J. Lippincott-Schwartz, *J. Cell Biol.* **155**, 557 (2001).
11. A. Girod et al., *Nature Cell Biol.* **1**, 423 (1999).
12. B. Storrie et al., *J. Cell Biol.* **143**, 1505 (1998).
13. S. Miles, H. McManus, K. E. Forsten, B. Storrie, *J. Cell Biol.* **155**, 543 (2001).
14. Time-lapse phase images were acquired at 1-min inter-

## REPORTS

biofilm formation (1, 2) and mediate binding to a variety of host proteins (3–5).

Polymerized curli appear as 4- to 7-nm-wide fibers of varying lengths by negative-stain electron microscopy (EM) (6). Under high-resolution EM, curli appeared as a tangled and amorphous matrix surrounding the bacteria (Fig. 1A) (7). At higher magnifications, curli fibers appeared as ~6- to 12-nm-

wide fibers of varying lengths (Fig. 1, B and C).

Curli were purified from MC4100 by sequential differential centrifugation (S6) and analyzed by SDS-polyacrylamide gel electrophoresis (PAGE) (8). Resolution of CsgA, the major structural component of curli, required brief treatment with 90% formic acid (FA) to depolymerize the CsgA polymers into a ~17.5-kD protein and two minor proteins that migrated at ~30 and 32 kD (Fig. 1D). Only the 17.5- and 32-kD bands were unique to FA-treated samples, and these bands were recognized by antibodies to CsgA (anti-CsgA) (9). The migration of these proteins is consistent with monomer and dimer sizes of CsgA (10, 11). By EM, non-FA-treated S6 curli were indistinguishable from those presented naturally on the bacterial surface, appearing as aggregated fibers of vary-

ing lengths and widths (compare Fig. 1, E and F). Circular dichroism (CD) analysis indicated that these fibers were rich in  $\beta$ -sheet secondary structure with a minimum peak at ~218 nm (Fig. 2A).

Like other amyloid fibers, S6 curli induced a spectral change of a 10  $\mu$ M Congo red (CR) solution with a maximum difference in absorbance between CR alone and CR bound to curli fibers at ~541 nm (Fig. 2, B and C) (12). The curli used in these assays contained a small amount of contaminating proteins (Fig. 1D). Pure, intact curli (called GP curli for "gel-purified") were isolated as described (10) (Fig. 1D). GP curli retained the ability to bind CR and cause the red shift, demonstrating that curli were sufficient to augment the absorbance of CR (Fig. 2B). Addition of purified S6 curli to a 5  $\mu$ M solution of thioflavin T (ThT) resulted in a fluorescence emission maximum at 482 nm (Fig. 2D), which is identical to the fluorescence induced by other amyloid proteins (13, 14).

Amyloid formation in eukaryotic cells is thought to be the result of a misguided protein-folding pathway. In contrast, *E. coli* possesses a specific nucleation-precipitation machinery encoded by the *csgAB* and *csgDEFG* operons to assemble curli. CsgB is thought to nucleate CsgA fibers (15). The *csgDEFG* genes encode CsgD, a FixJ-like transcriptional regulator, and three putative curli assembly factors, CsgE, CsgF, and CsgG. The lipoprotein CsgG localizes to the inner leaflet of the outer membrane and may serve as a curli assembly platform (16).

A nonpolar *csgF*<sup>-</sup> deletion mutant (MHR592) (17) resulted in aberrant CR binding properties. Wild-type bacteria stained CR-positive after 30 hours of growth on YESCA plates (9). Strain MHR592 (*csgF*<sup>-</sup>) was CR-negative after 30 hours of growth and only slightly CR-positive after 48 hours of growth (9). EM analysis of *csgF*<sup>-</sup> bacteria showed that fibers were less abundant but were otherwise indistinguishable from those produced by wild-type bacteria (Fig. 3A).

The monomeric and polymeric state of CsgA in the absence of CsgF was assessed. Very little SDS-soluble CsgA was present in extracts made from wild-type bacteria (Fig. 3B) because most of the CsgA subunits were assembled into curli as determined by the presence of a 17.5-kD band after pretreatment with FA (Fig. 3B). Similar to a *csgB*<sup>-</sup> mutant (Fig. 3B), most CsgA produced by a *csgF*<sup>-</sup> mutant remained in an SDS-soluble form after 48 hours of growth (Fig. 3B).

CsgA is secreted in a soluble, assembly-competent form by a *csgB*<sup>-</sup> mutant (*CsgA*<sup>-</sup> donor) and can be assembled on the surface of *csgA*<sup>-</sup> mutant (*CsgB*<sup>+</sup> recipient) bacteria in a process called interbacterial complementation (Fig. 3D) (18). *CsgB*<sup>-</sup> recipient cells lacking the CsgA protein stained CR-positive when

<sup>1</sup>Department of Molecular Microbiology and Microbial Pathogenesis, Box 8230, <sup>2</sup>Department of Cell Biology and Physiology, Box 8228, Washington University School of Medicine, 660 South Euclid Avenue, St. Louis, MO 63110, USA. <sup>3</sup>Department of Microbiology and Tumorbiology Center (MTC), Karolinska Institute, Box 280, S-171777 Stockholm, Sweden.

\*To whom correspondence should be addressed. E-mail: hultgren@borcim.wustl.edu

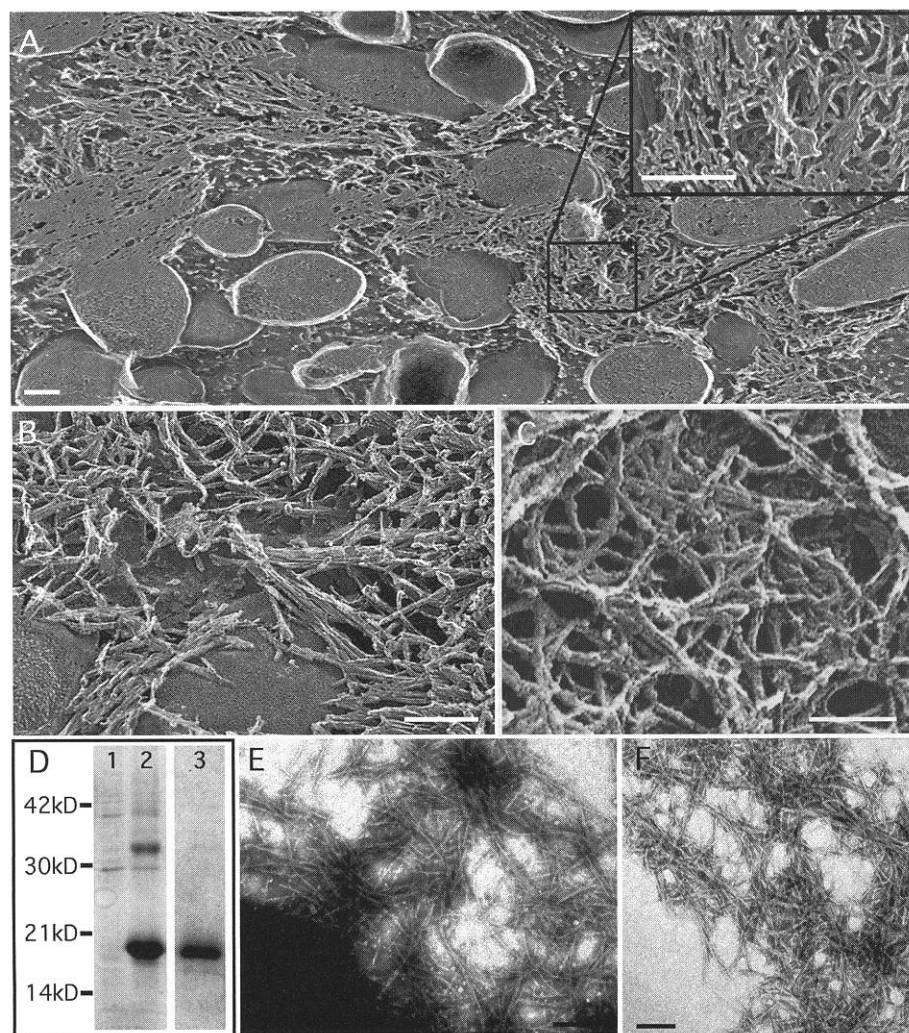


**Fig. 1.** High-resolution deep-etch EM micrographs of curliated *E. coli* and purification of curli fibers. (A and B) Representative freeze-fractured micrographs that have been rotary shadowed with platinum. The inset in (A) shows curli fibers. (C) MC4110 was absorbed onto glass and deep-etched without being fractured before rotary shadowing with platinum. (D) Coomassie stain SDS-PAGE of curli samples isolated from *E. coli* strain MC4100. Lanes 1 and 2 contain 40  $\mu$ g of S6 wild-type curli without and with FA treatment, respectively. Lane 3 contains 20  $\mu$ g of FA-treated GP curli. Molecular size markers (in kilodaltons) are indicated on the left. (E) Negative-stain EM micrographs of MC4100 grown on YESCA plates at 26°C for 48 hours. (F) Negative-stain EM micrograph of purified wild-type S6 curli. Bars: (A), 400 nm; (B) and (C), 60 nm; (E) and (F), 200 nm.

REPORTS

cross-streaked with either *csgF*<sup>-</sup> or *csgF*<sup>-</sup>*B*<sup>-</sup> double-mutant bacteria (Fig. 3D), indicating that CsgA was secreted from *csgF*<sup>-</sup> cells and assembled on the CsgB<sup>+</sup> recipient cells. In contrast, *csgF*<sup>-</sup> and *csgF*<sup>-</sup>*B*<sup>-</sup> mutants were unable to accept CsgA from a CsgA<sup>+</sup>-donating strain (Fig. 3D). Thus, the curli assembly defect in *csgF*<sup>-</sup> mutants was a nucleation defect because CsgA produced by these cells was assembly competent. CsgF may work independently or in concert with CsgB to guide in vivo extracellular nucleation of CsgA.

A nonpolar *csgE*<sup>-</sup> deletion mutant (MHR480) (17) produced pale, non CR-binding colonies similar to those produced by a *csgA* mutant (9). Despite the pale-colony phenotype, MHR480 (*csgE*<sup>-</sup>), but not a *csgE*<sup>-</sup>*A*<sup>-</sup> double mutant, produced fibers that reacted with anti-CsgA. However, these structures were less abundant than wild-type curli and were architecturally distinct in that they tended to arrange into rings (Fig. 3C). In the *csgE*<sup>-</sup> cells, no SDS-soluble CsgA could be detected, and the total amount of SDS-insoluble CsgA was markedly reduced (CsgA was detected in the FA-treated sample only after extended exposure) (Fig. 3B). A *csgE*<sup>-</sup> mutant was unable to donate CsgA subunits when cross-streaked against the CsgB<sup>+</sup> recipient (Fig. 3D). However, a *csgE*<sup>-</sup> mutant retained the ability to act as a recipient and guide CsgA polymerization, because it stained CR-positive when cross-streaked against a CsgA<sup>+</sup> donor (Fig. 3D). This staining was weaker than that observed on a CsgB<sup>+</sup> recipient cross-streaked against a CsgA<sup>+</sup> donor (Fig. 3D), suggesting that in addition to the CsgA stability defect, *csgE*<sup>-</sup> bacteria are also partially defective in their ability to nucleate exogenous CsgA. A *csgB*<sup>-</sup>*E*<sup>-</sup> double mutant was unable to accept or donate CsgA (Fig. 3D).

To understand the requirements for subunit polymerization, we purified CsgA in a soluble form and analyzed its polymerization in vitro. A six-histidine-tagged version of *csgA* (CsgA-his) was cloned behind the IPTG (isopropyl-β-D-thiogalactopyranoside)-inducible *trc* promoter in pHL3 (17), to create pMC3 (19). Plasmid-derived CsgA-his complemented fiber formation and CR binding in a *csgA*<sup>-</sup> mutant (9). To produce soluble, nonpolymerized CsgA, we transformed pMC3 (*csgA*-his) into LSR6 (C600:Δ*csgDEFG*;Δ*csgBA*) (19). However, attempts to detect CsgA-his protein expressed in LSR6 were unsuccessful (Fig. 4A). When LSR6/pMC3 (*csgA*-his) was transformed with pMC5 (*csgEFG*) or pMC1 (*csgG*), CsgA-his could be detected in the culture supernatants (Fig. 4A). Under these growth conditions (logarithmic growth in LB broth), only CsgG, and not CsgE, was required for efficient CsgA stabilization and secretion.

CsgA-his was purified from the supernatant of LSR6/pMC3/pMC5 and LSR6/pMC3/pMC1 by standard nickel affinity chromatogra-

Fig. 2. Amyloid-like properties of curli. (A) The CD spectrum of wild-type S6 curli was measured with 300 μg of protein in 10 mM tris (pH 7.4) with a 0.02-cm cell in a JASCO J715 spectropolarimeter at 25°C. S6 and GP curli gave similar CD spectra. (B) A 10-μM solution of CR prepared in 10 mM tris (pH 7.4) and 100 mM NaCl was filtered through a 0.2-μm filter and mixed with 50 μl of buffer [10 mM tris (pH 7.4)] (◆), S6 curli (4 mg/ml stock) (○), or GP curli (4 mg/ml stock) (×) in a final volume of 1 ml. All spectra were normalized against the relevant non-CR-containing solutions. (C) Spectra representing the difference of CR with S6 curli and CR alone. (D) Fluorescence of 5 μM ThT alone (◇) or mixed with 40 μg of S6 curli (○) after excitation at 450 nm on an AlphaScan PTI fluorometer with a slit width of 4 nm. GP and S6 curli gave indistinguishable fluorescence results.

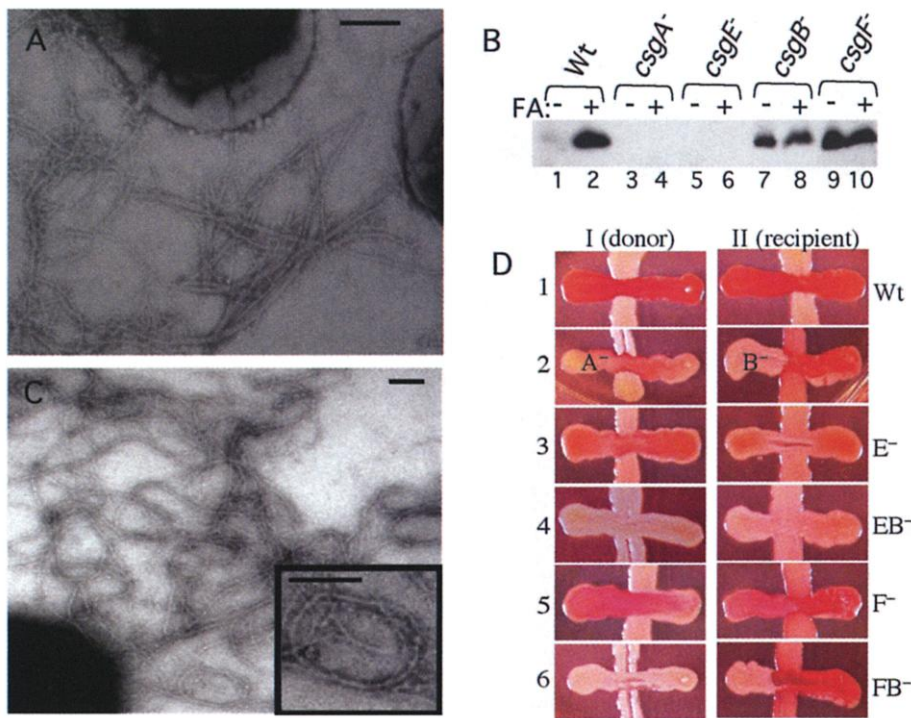
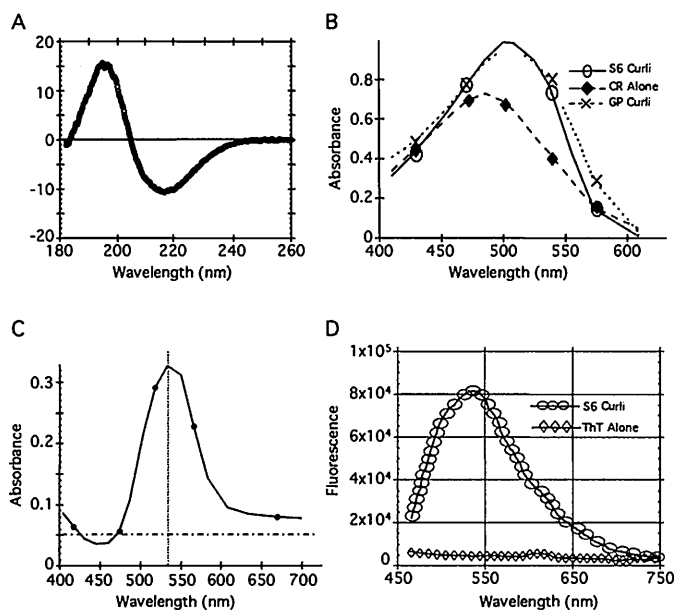


Fig. 3. Curli biogenesis in the absence of CsgE and CsgF. (A) Negative-stain EM micrographs of MHR592 (*csgF*<sup>-</sup>) bacteria grown on YESCA plates at 26°C for 48 hours. (B) CsgA visualized by Western analysis with anti-CsgA (16) and bacteria grown at 26°C on YESCA plates for 48 hours. Circular plugs of 8 mm, including cells and underlying agar (to collect soluble, unpolymerized and secreted CsgA), were collected and resuspended in 200 μl of 1.5× SDS loading buffer either with or without prior FA treatment. The extracts loaded in each lane are as follows: lanes 1 and 2, MC4100 (wild type); lanes 3 and 4, LSR10 (*csgA*<sup>-</sup>); lanes 5 and 6, MHR480 (*csgE*<sup>-</sup>); lanes 7 and 8, MHR261 (*csgB*<sup>-</sup>); and lanes 9 and 10 MHR592 (*csgF*<sup>-</sup>). (C) Negative-stain EM micrographs of MHR480 (*csgE*<sup>-</sup>) bacteria grown on YESCA plates at 26°C for 48 hours. These fibers often looped into imperfect circles (see inset). (D) Interbacterial complementation and CR binding in *csgE*<sup>-</sup> and *csgF*<sup>-</sup> mutants. The CsgA<sup>+</sup> donor strain MHR261 (I) and the CsgB<sup>+</sup> recipient strain LSR10 (II) were streaked from the top of the plate to the bottom. The horizontal cross-streaks were made from left to right with the following strains: MC4100 (wild type) (I-1 and II-1), *csgA*<sup>-</sup> (I-2), *csgB*<sup>-</sup> (II-2), *csgE*<sup>-</sup> (I-3 and II-3), *csgEB*<sup>-</sup> (I-4 and II-4), *csgF*<sup>-</sup> (I-5 and II-5), and *csgFB*<sup>-</sup> (I-6 and II-6). Bars in (A) and (C), 200 nm.

phy (Fig. 4B). Immediately after elution from the nitrilotriacetic acid (NTA) agarose column, solutions containing purified CsgA-his were clear with no evidence of aggregation, and EM of this material revealed no fibers (9). CD analysis of this material indicated that soluble CsgA-his, unlike curli, was not rich in  $\beta$ -sheet secondary structure (Fig. 4C). However, after prolonged incubation (4°C for 4 to 12 hours), the CsgA-his solutions became opaque and noticeably viscous. EM analysis revealed that fibers had formed that were similar to those produced by wild-type bacteria (Fig. 4D). The *in vitro*-assembled CsgA-his fibers, but not the CsgA-his soluble precursors, were able to bind CR and cause a red shift (Fig. 4E), signifying that they had adopted the cross  $\beta$  structure conserved in all amyloid fibers. CsgA purified from cells expressing *csgEFG* or only *csgG* formed CR-binding fibers with indistinguishable kinetics (9). Thus, although CsgB and

CsgEFG are required to facilitate efficient polymerization *in vivo*, they are not required for polymerization to proceed under these *in vitro* conditions. A critical function of the nucleation-precipitation assembly machinery may be to prevent CsgA polymerization within the cell and accelerate it at the cell surface.

Our demonstration that *E. coli* can produce extracellular amyloid-like fibers increases the recognized functional repertoire of amyloid fibers and provides a useful model system to study their formation. Purified amyloid fiber subunits associated with human diseases, such as the A $\beta$  protein associated with Alzheimer's disease, readily polymerize when incubated at high concentrations *in vitro* (20). However, the accessory proteins and conditions that facilitate *in vivo* polymerization of A $\beta$  are incompletely understood. Understanding the regulation of curli subunit polymerization in *E. coli* will offer insight

into the formation of eukaryotic amyloids. This work also raises the intriguing possibility that bacterial amyloids could play a role in certain human neurodegenerative and amyloid-related diseases. Future experiments will further examine the role of CsgB, CsgE, and CsgF during the *in vivo* polymerization of curli, and their function will be used as a model to understand the formation of other amyloids.

References and Notes

- O. Vidal et al., *J. Bacteriol.* **180**, 2442 (1998).
- J. W. Austin, G. Sanders, W. W. Kay, S. K. Collinson, *FEMS Microbiol. Lett.* **162**, 295 (1998).
- U. Sjöbring, G. Pohl, A. Olsen, *Mol. Microbiol.* **14**, 443 (1994).
- A. Olsen, A. Armqvist, M. Hammar, S. Normark, *Infect. Agents Dis.* **2**, 272 (1993).
- A. Ben Nasr, A. Olsen, U. Sjöbring, W. Muller-Esterl, L. Björck, *Mol. Microbiol.* **20**, 927 (1996).
- A. Olsen, A. Jonsson, S. Normark, *Nature* **338**, 652 (1989).
- MC4100 was grown on YESCA plates at 26°C for 50 hours, washed with 1 $\times$  phosphate-buffered saline, placed on aldehyde-fixed slices of rabbit lung, and then quickly frozen by abruptly pressing the samples against a copper block cooled to 4 K with liquid helium. Frozen samples were fractured (where indicated), then deep-etched by exposure to a vacuum for 2.5 min, and replicas were made by rotary shadowing with a mixture of platinum and carbon (27).
- MC4100 was spread as a lawn on 10 150-mm YESCA plates and grown at 26°C for 60 hours before being scraped from the plates and suspended in 300 ml of 10 mM tris (pH 7.4). Bacteria were blended five times on ice with an Omni-Mixer homogenizer for 1 min at 3-min intervals. The bacteria were pelleted by centrifuging two times at low speed (5000g, 10 min). The supernatant was made 150 mM NaCl and the curli pelleted by centrifuging at 13,000g. The pellet was resuspended in 300 ml of 10 mM tris (pH 7.4), 150 mM NaCl, and incubated on ice for 30 min before being centrifuged at 13,000g. This procedure was repeated three times. The pellet was then resuspended in 30 ml of 10 mM tris (pH 7.4) and pelleted as described above. The pellet was again suspended in 30 ml of 10 mM tris (pH 7.4) and centrifuged at 35,000g. For the gel-purified curli, 2.5 ml of the S6 fraction was mixed with an equal amount of 2 $\times$  SDS loading buffer and subjected to electrophoresis for 5 hours on a 12% SDS-PAGE gel. The curli remaining in the slot after electrophoresis were recovered as described (10).
- M. R. Chapman, L. S. Robinson, S. J. Hultgren, unpublished observations.
- S. K. Collinson, L. Emody, K. H. Muller, T. J. Trust, W. W. Kay, *J. Bacteriol.* **173**, 4773 (1991).
- A. Olsen, A. Armqvist, M. Hammar, S. Sukupolvi, S. Normark, *Mol. Microbiol.* **7**, 523 (1993).
- W. E. Klunk, R. F. Jacob, R. P. Mason, *Methods Enzymol.* **309**, 285 (1999).
- H. LeVine III, *Methods Enzymol.* **309**, 274 (1999).
- H. LeVine, *Protein Sci.* **2**, 404 (1993).
- Z. Bian, S. Normark, *EMBO J.* **16**, 5827 (1997).
- H. Loferer, M. Hammar, S. Normark, *Mol. Microbiol.* **26**, 11 (1997).
- M. Hammar, Karolinska Institute (1997).
- \_\_\_\_\_, Z. Bian, S. Normark, *Proc. Natl. Acad. Sci. U.S.A.* **93**, 6562 (1996).
- MC4100 chromosomal DNA was amplified with the primers 5'-CATATGAACTTTTAAAGTAGCAGCAATG and 5'-GAATCTAATGGTGATGGTATGGTGGTACTGATGAGGATCC, and the amplicon was cloned into the Nde I and Eco RI sites of pHL3 to create pMC3 by standard techniques. The *csgEFG* genes were similarly amplified and cloned into the Nco I and Bam HI sites of pTrc99A to create pMC5 (Pharmacia, Piscataway, NJ) with the primers 5'-CCATGGCGAAACGT-TATTTACGCTG and 5'-GGATCCTCAGGATTCGGTGGAAACCGAC. Knockouts of *csgA* or of the entire curli locus were made by homologous recombination as described (22). The *kan<sup>r</sup>* cassette from pKD13 was am-

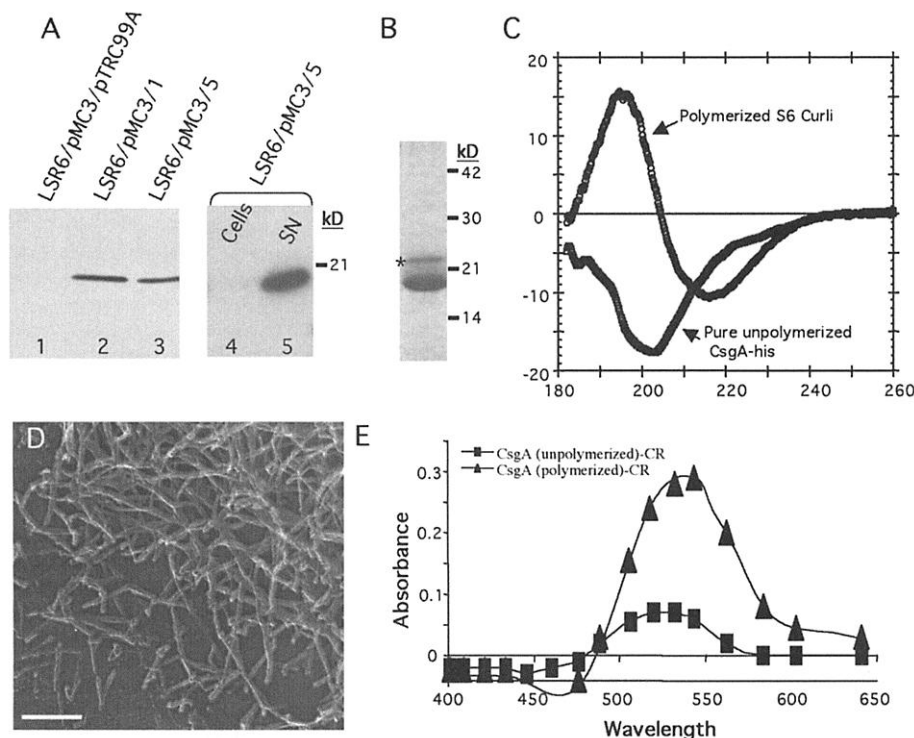


**Fig. 4.** Purification and *in vitro* assembly of CsgA-his. (A) Western blot with anti-his (Covance, Richmond, California) to determine expression and cellular location of overexpressed CsgA-his. Log-phase cultures containing (lane 1) pMC3 (*csgA-his*) and pTrc99A (empty vector); (lane 2) pMC3 and pMC1 (*csgG*); or (lane 3) pMC3 and pMC5 (*csgEFG*) were induced with 0.5 mM IPTG for 1 hour; samples were removed and mixed with an equal amount of 2 $\times$  SDS-PAGE dye and heated to 95°C before gel electrophoresis. CsgA-his expression with pTrc99A was detected only after overexposure of the blot. The cellular and supernatant fractions from cultures containing pMC3 and pMC5 were separated by centrifugation and loaded in lanes 4 and 5, respectively. (B) CsgA-his was purified from cleared LSR6/pMC3/pMC5 supernatants filtered through a 0.2- $\mu$ m filter before loading on a disposable column packed with nickel NTA-agarose beads (Qiagen, Chatsworth, California). The column was washed with 10 column volumes of 10 mM tris (pH 7.4), 100 mM NaCl, and CsgA-his was eluted with 5 ml of wash buffer plus 100 mM imidazole and analyzed by Coomassie stain SDS-PAGE. Both the major band migrating at  $\sim$ 17.5 kD and the higher molecular weight, minor band (indicated by an asterisk) interacted with anti-CsgA (9). (C) The CD spectrum of wild-type S6 curli compared with that of 300  $\mu$ g of soluble unpolymerized CsgA-his assayed immediately after purification. (D) High-resolution EM of pure CsgA-his preparations after a 1-week incubation at 4°C. Bar, 140 nm. (E) Absorbance of a 10  $\mu$ M solution of CR with 100  $\mu$ g of pure, unpolymerized CsgA-his (■) or pure polymerized CsgA-his (▲) after subtracting the absorbance of CR alone.

plified by polymerase chain reaction (PCR) with primers containing 5'-homology arms corresponding to sequences flanking the regions to be deleted. Primers used to create LSR10 ( $\Delta csgA$ ) were 5'-gttaattccattcgacttt-aaatcaatccgatgggggttttacGTGATAGGCTGGAGCTGCTTC and 5'-agggtctgcgcctgtttctgtaatacaaatgatgtATCCGGGATCCGTCGACC (lower-case letters correspond to *csg* sequences). The primers used to generate LSR5 ( $\Delta csgDEF; \Delta csgBA$ ), were 5'-agggtctgcgcctgtttctgtaatacaaatgatgtATCCGGGATCCGTCGACC and 5'-gcc-gacatcaggcacagcataacagggttcgttcgagGTGATAGGCTGG-

AGCTGCTTC. PCR products were electroporated into MC4100-expressing Red recombinase proteins from pKD46 (22). The resulting Kan<sup>r</sup> strains were confirmed by PCR and failed to bind CR when grown on YESCA plates. The mutation from LSR5 was transferred into C600 by standard P1 transduction, creating LSR6.

20. C. J. Barrow, A. Yasuda, P. T. Kenny, M. G. Zagorski, *J. Mol. Biol.* **225**, 1075 (1992).  
 21. J. E. Hueser, *J. Muscle Res. Cell Motil.* **8**, 303 (1987).  
 22. K. A. Datsenko, B. L. Wanner, *Proc. Natl. Acad. Sci. U.S.A.* **97**, 6640 (2000).

23. We thank members of the Hultgren lab and especially K. Dodson for helpful comments during the preparation of this manuscript. This work was supported by the Alzheimer's Disease Research Center grant NIA P50 AG05681-17 and NIH grants AI29549, DK51406, and AI48689 (S.J.H.). S.N. acknowledges grants from the Swedish Medical Research Council (16x-10843) and Swedish Natural Science Research Council (3373-309). M.R.C. was supported by a Keck fellowship and by NIH fellowship 1 F32 AI10502-01A1.

29 October 2001; accepted 7 December 2001

# A Role for Interaction of the RNA Polymerase Flap Domain with the $\sigma$ Subunit in Promoter Recognition

Konstantin Kuznedelov,<sup>1\*</sup> Leonid Minakhin,<sup>1\*</sup>  
 Anita Niedziela-Majka,<sup>2,†</sup> Simon L. Dove,<sup>3</sup> Dragana Rogulja,<sup>1</sup>  
 Bryce E. Nickels,<sup>3</sup> Ann Hochschild,<sup>3</sup> Tomasz Heyduk,<sup>2</sup>  
 Konstantin Severinov<sup>1,§</sup>

In bacteria, promoter recognition depends on the RNA polymerase  $\sigma$  subunit, which combines with the catalytically proficient RNA polymerase core to form the holoenzyme. The major class of bacterial promoters is defined by two conserved elements (the  $-10$  and  $-35$  elements, which are 10 and 35 nucleotides upstream of the initiation point, respectively) that are contacted by  $\sigma$  in the holoenzyme. We show that recognition of promoters of this class depends on the "flexible flap" domain of the RNA polymerase  $\beta$  subunit. The flap interacts with conserved region 4 of  $\sigma$  and triggers a conformational change that moves region 4 into the correct position for interaction with the  $-35$  element. Because the flexible flap is evolutionarily conserved, this domain may facilitate promoter recognition by specificity factors in eukaryotes as well.

At most bacterial promoters, RNA polymerase (RNAP) holoenzyme ( $\alpha_2\beta\beta'\omega\sigma$ ) recognizes sequence elements centered  $\sim 10$  and  $\sim 35$  nucleotides upstream of the initiation point, with the  $\sigma$  subunit specifically contacting both promoter elements [reviewed in (1)]. Different sigmas share four evolutionarily conserved regions, which can be further subdivided (1). Centrally located region 2.4 interacts with the  $-10$  promoter element, and COOH-terminal region 4.2 interacts with the  $-35$  element (1). Because most free  $\sigma$  subunits cannot recognize

promoters, conformational changes in core RNAP,  $\sigma$ , or both must occur during holoenzyme formation. Indeed, luminescence resonance energy transfer (LRET) measurements show that the *Escherichia coli* RNAP core induces a change in  $\sigma^{70}$ , the principal  $\sigma$  (2). As a result, the distance between  $\sigma^{70}$  regions 2.4 and 4.2 increases dramatically, to match the distance between the promoter elements (2). The mechanism by which the conformation of  $\sigma$  is altered upon holoenzyme formation has not been defined, nor have the core interaction sites that bring about this change been identified.

A structure of core RNAP from eubacterium *Thermus aquaticus* has been determined (3). One structural element, the "flexible flap" (comprising conserved segment G of the RNAP  $\beta$  subunit), protrudes away from the body of the enzyme (Fig. 1). An *E. coli* RNAP mutant lacking  $\beta$  amino acids 900 through 909 at the tip of the flap was previously found to be defective in transcription initiation unless the initiation region was premelted (4). To further examine this defect, we deleted the entire flap from *E. coli* RNAP (5). Inspection suggests that the RNAP struc-

ture should be minimally perturbed by the deletion (Fig. 1).

Mutant RNAP was purified (6), and the ability of mutant holoenzyme ( $E\sigma^{70}$ ) to initiate transcription from T7 A2, a strong  $-10/-35$  promoter, was tested (7). Wild-type  $E\sigma^{70}$  was active at T7 A2; in contrast, mutant  $E\sigma^{70}$  was inactive (Fig. 2A). Transcription from the *galP1* promoter was also tested. This promoter belongs to a class of promoters whose  $-10$  elements are extended by an upstream dinucleotide TG (8).  $\sigma$  region 4.2 is not required for recognition of extended  $-10$  promoters, due to additional RNAP contacts with the TG motif (8).  $E\sigma^{70}$  lacking the  $\beta$ -flap was active at *galP1* (Fig. 2A). These results suggest that the  $\beta$ -flap is important for transcription from  $-10/-35$  promoters, but is dispensable for transcription from extended  $-10$  promoters.

Wild-type  $E\sigma^{70}$  protected T7 A2 promoter DNA from deoxyribonuclease I (DNase I) digestion (Fig. 2B) (7). In contrast, the pattern of DNase I digestion in reactions containing mutant  $E\sigma^{70}$  was similar to the naked DNA pattern, suggesting that  $E\sigma^{70}$  lacking the  $\beta$ -flap is unable to form complexes with  $-10/-35$  promoters.

The restricted promoter specificity caused by the  $\beta$ -flap deletion could be direct (i.e., the flap contributes directly to promoter recognition) or indirect (i.e., the flap positions  $\sigma$  region 4.2 for interaction with the  $-35$  element). The following experiments support the second possibility. We studied  $\sigma^{70}$  region 4.2-DNA interactions in *galP1* complexes, where region 4.2 makes favorable, but nonessential DNA interactions  $\sim 35$  base pairs (bp) upstream of the initiation point (8). Overall, the *galP1* complexes formed by mutant  $E\sigma^{70}$  appeared similar to the wild-type complexes (Fig. 2C) (8). However, DNA between positions  $-34$  and  $-39$  was protected in the wild-type, but not in the mutant complexes (Fig. 2C, arrowheads), suggesting that in the absence of the  $\beta$ -flap, interactions between  $\sigma$  region 4.2 and *galP1* upstream DNA do not occur.

To show directly that the  $\beta$ -flap is required for the conformational change in  $\sigma$  that occurs upon holoenzyme formation, we used LRET, which uses energy transfer between a luminescent donor and fluorescent acceptor to determine atomic-scale distances between the probes (9). LRET donor and acceptor probes were incorporated into different  $\sigma$  domains, and inter-

<sup>1</sup>Waksman Institute, Department of Genetics, Rutgers University, Piscataway, NJ 08854, USA. <sup>2</sup>E. A. Doisy Department of Biochemistry and Molecular Biology, St. Louis University Medical School, St. Louis, MO 63104, USA. <sup>3</sup>Harvard Medical School, Department of Microbiology and Molecular Genetics, Boston, MA 02115, USA.

\*These authors contributed equally to this work.

†On leave from Limnological Institute of the Russian Academy of Sciences, Irkutsk, Russia.

‡On leave from Department of Organic Chemistry, Biochemistry and Biotechnology, Wrocław University of Technology, Wrocław, Poland.

§To whom correspondence should be addressed. E-mail: severik@waksman.rutgers.edu